# Inhibition Effectiveness of Laser-cleaned Nanostructured Aluminum Alloys to Sulfate-reducing Bacteria Based on Super-wetting and Ultra-slippery Surfaces

*Ze Tian[a], Zhenglong Lei[a,*], Yanbin Chen[a], Chuan Chen[b,*], Ruochen Zhang[b], Xi Chen[a], Jiang Bi[a], Haoran Sun[a]*

a State Key Laboratory of Advanced Welding and Joining, Harbin Institute of Technology, Harbin, 150001, China

b State Key Laboratory of Urban Water Resource and Environment, School of Environment, Harbin Institute of Technology, Harbin, Heilongjiang Province 150090, China
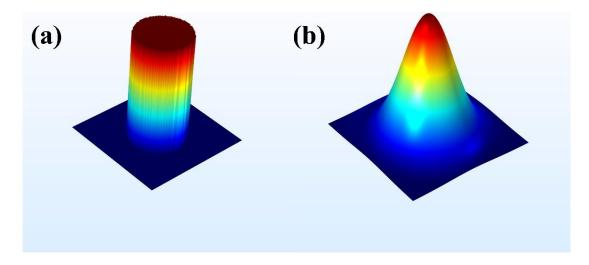
* Corresponding authors

*E-mail: leizhenglong@hit.edu.cn (Zhenglong Lei)

*E-mail: echo110244@126.com (Chuan Chen)

The overlapped rate can be expressed as follows:

$$\varphi = \frac{D - d}{D} \qquad (1)$$

where $D$ refers to the diameter of laser spot, $d$ refers to the scanning interval. The schematic representation of the laser cleaning scanning path is shown in our previous work.[1]



**Figure S1.** Laser energy distribution mode (a) top-hat laser used in this work (b) Gaussian laser used in other fast-laser (~ns) micromachining references.
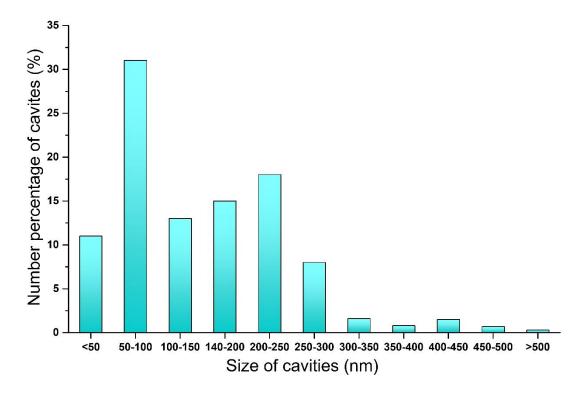
**Figure S2.** Estimated number percentage of cavities for the nanostructured layer of SI2.
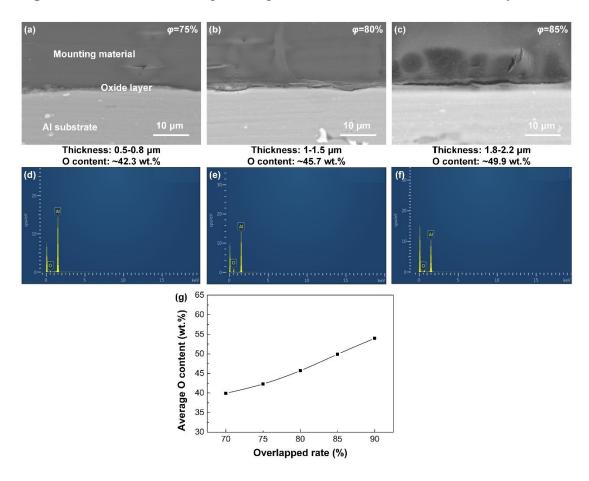
**Figure S3.** The cross-sectional morphology SEM images of the samples at the overlapped rates of 75 % (a), 80 % (b), and 85 % (c). EDS spectra of O content at the overlapped rates of 75 % (d), 80 % (e), and 90 % (f). The curve of oxygen content *vs.* the overlapped rate (g).
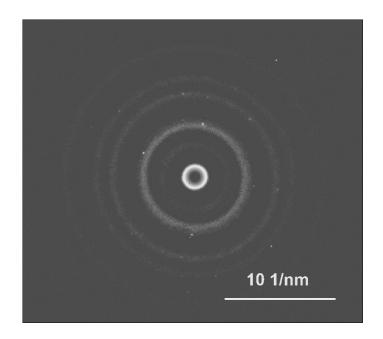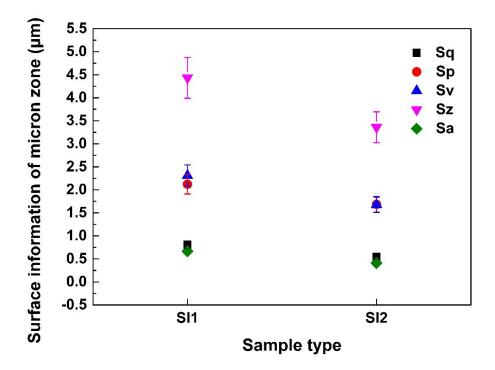


**Figure S4.** The processed image of Figure 5b.

**Figure S5.** Surface information of micron-zone (60 μm × 60 μm) of SI1 and SI2. $S_a$ refers to the arithmetical mean deviation. $S_q$ refers to the root mean squared. $S_v$ refers to the maximum valley depth. $S_p$ refers to the maximum peak height. $S_z$ refers to the maximum height of the profile.
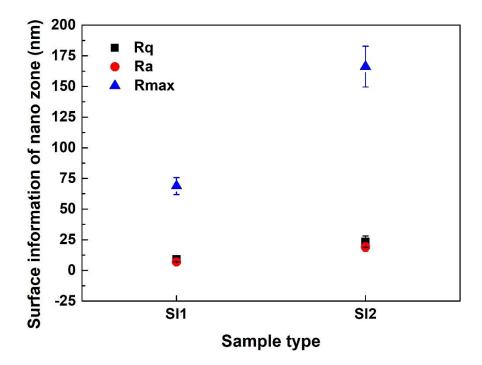
**Figure S6.** Surface information of nano-zone (1000 nm × 1000 nm) of SI1 and SI2. $R_a$ refers to the arithmetical mean deviation. $R_q$ refers to the root mean squared. $R_{max}$ refers to the maximum height of the profile.
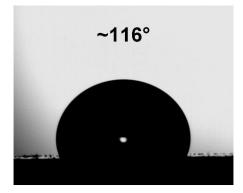


**Figure S7.** Contact angle of the fluorinated polished original Al substrate.

The water contact angle was directly controlled by the area fraction of the solid-liquid interface and air-liquid interface. The relationship between the water contact angle and
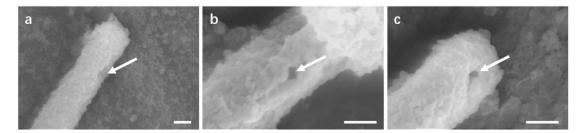
the area fraction can be expressed as **Eq (2)**.

$$\cos\theta_r = f_{sl}\cos\theta_{sl} + f_{gl}\cos\theta_{gl} \tag{2}$$

Where $\theta_r$, $\theta_{sl}$ refer to the water contact angles of the fluorinated laser-cleaned surface and fluorinated Al substrate, $\theta_{gl}$ refers to the contact angle of liquid and air. Contact area fraction $f$ is defined as the ratio of the actual area of solid/liquid and air/liquid interface, thus $f_{sl}$ and $f_{gl}$ refer to the area fraction of the solid/liquid interface and the air/liquid interface. As a result of $f_{sl} + f_{gl} = 1$, Eq (2) can be induced from **Eq (2)**.

$$f_{gl} = \frac{\cos\theta_{sl} - \cos\theta_r}{\cos\theta_{sl} + 1} \tag{3}$$

Hence, the contact area fraction of liquid/air can be calculated according to the **Eq (2)**. It implies that the air prevents the penetration of water into the gaps among nanostructures on the surfaces under the condition of Cassie-Baxter state, and the area fraction value of the air that occupies between the liquid and the surfaces was $f_{gl}$.



**Figure S8.** Typical nanopores and trumpet-shaped portals on the cell surface. (a), (b), and (c) are three different SEM images. (Scale bar is 200 nm)
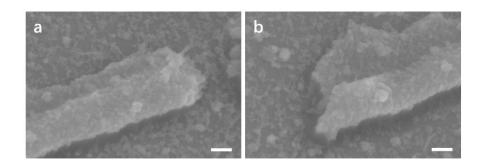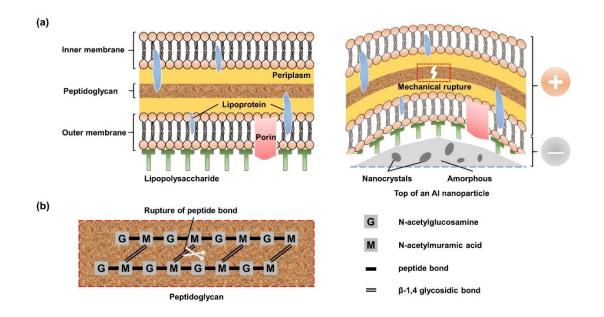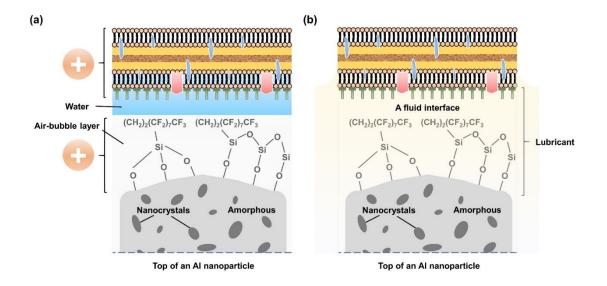
**Figure S9**. Morphology of the broken cells that were cut open. (a) and (b) are two different broken cells. (Scale bar is 200 nm)



**Figure S10.** Anti-bacterial mechanism of the superhydrophilic surface. Structures of the cell wall before and after the role of Al nanoparticle from superhydrophilic surfaces (a), rupture of the peptide bond within the interior of peptidoflycan (b).

**Figure S11.** Anti-adhesion mechanism of the superhydrophobic surface (a) and ultra-slippery surface (b).
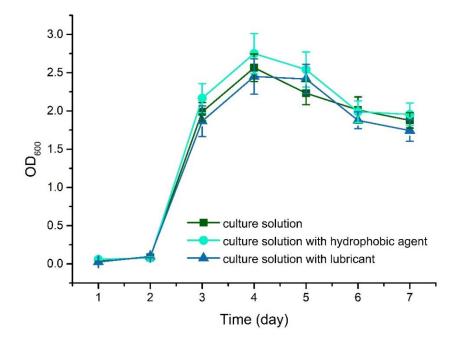


**Figure S12**. Growth curves of SRB in culture solution, with PFTEOS and with PFPE.

Definition of relative biofilm/bacterial/microorganism attachment RA:

$$RA = \frac{Coverage_{SLIPS}}{Coverage_{Control}} = \frac{Total\ cell\ number_{SLIPS}}{Total\ cell\ number_{Control}}$$

**Table S1** Relative cell attachment on the SLIPSs (%)

| | Substrate | Fouling species | Immersion duration (day) | Relative attachment (%) |
|---|---|---|---|---|
| 1[2] | polytetrafluoroethylene | *Pseudomonas aeruginosa* | 7 | 0.40 |
| 2[3] | glass | *C. reinhardtii* | 8 | 7.10 |
| 3[4] | aluminum | *Desulfovibrio sp.* | 14 | 0.20 |
| 4[5] | glass | *Desulfovibrio sp.* | 10 | 5.00 |
| 5 | aluminum | *Desulfovibrio desulfuricans subsp. desulfuricans* | 14 | 0.05 |

# Reference

(1) Tian, Z.; Lei Z. L.; Chen X.; Chen Y. B.; Zhang L. C.; Jiang B.; Liang J. W. Nanosecond pulsed fiber laser cleaning of natural marine micro-biofoulings from the surface of aluminum alloy. *J. Clean. Prod.* **2019**, 244, 118724.

(2) Epstein, A. K.; Wong, T. S.; Belisle, R. A.; Boggs, E. M.; Aizenberg, J.; *Proc. Natl. Acad. Sci. U. S. A.* **2012**, 109, 13182–13187.

(3) Tesler, A. B.; Kim, P.; Kolle, S.; Howell, C.; Ahanotu, O.; Aizenberg J. *Nat. Commun.* **2015**, 6, 8649.

(4) Wang, P.; Zhang, D.; Lu, Z.; Sun, S. M. Fabrication of slippery lubricant-infused porous surface for inhibition of microbially influenced corrosion. *ACS Appl. Mater. Inter.* **2016**, 8, 2, 1120−1127.

(5) Wang, P.; Zhang, D.; Sun, S. M.; Li, T. P.; Sun, Y. Fabrication of slippery lubricant-infused porous surface with high underwater transparency for the control of marine biofouling. *ACS Appl. Mater. Inter.* **2017**, 9, 1, 972−982.